

## Corrosion Inhibition Efficiency of Modified Silver Nanoparticles For Carbon Steel in 1 M HCl

Ayman M Atta, G. A. El-Mahdy\* and Hamad A. Al-Lohedan

Chemistry department, College of Science, King Saud University, P.O.Box - 2455, Riyadh - 11451, Saudi Arabia

\*E-mail: [gamalmah2000@yahoo.com](mailto:gamalmah2000@yahoo.com)

Received: 30 January 2013 / Accepted: 28 February 2013 / Published: 1 April 2013

---

A simple method was applied to prepare coated silver nanoparticles with polymerizable surfactants. In this respect, Noigen R-N10 was modified by esterification with maleic anhydride. The produced surfactant was used as dispersing agent for silver nanoparticles, which prepared from AgNO<sub>3</sub>. The size and the morphology of the nanoparticles have been examined by conventional and high-resolution transmission electron microscopy. The prepared silver nanoparticles has size ranging from 25 to 80 nm, while the diameters ranging from 2 to 18 nm. The prepared silver nanoparticles have been employed as corrosion inhibitor for carbon steel in 1M HCl solution using electrochemical impedance spectroscopy (EIS) technique. EIS data indicated that silver nanoparticles reduced drastically the corrosion rate of carbon steel and exhibit good performance as well as barrier property against the corrosion in HCl solution.

---

**Keywords:** Carbon steel, Ag nanoparticles, TEM, EIS

### 1. INTRODUCTION

Nowadays, carbon steel has become an important part of our life due to its extensively applications in automotive, household appliances, petroleum, and heavy construction such as marine and chemical industries. It is selected for construction because of its mechanical properties and machine-ability at a low price, while at the same time; they have to be resisted against corrosion phenomena. This fact is one of the major reasons for industrial accidents and consuming of material resources [1, 2]. Acid solutions were widely used in industrial acid cleaning, acid descaling, acid picking and oil-well acidizing. In these acid solutions corrosion inhibitors are required in order to restrain the acid erosion of metallic materials [3]. In order to reduce the corrosion of metals, several techniques have been applied. The use of corrosion inhibitors is one of the most practical methods for

protection against corrosion in acidic media. Corrosion inhibitors can be classified into three kinds: (i) inorganic inhibitors, (ii) organic inhibitors, and (iii) mixed material inhibitors [4]. Several studies have examined the relationship between the structure of the inhibitor molecule and its efficiency [5-9] but much less attention has been paid to the dependence of the protection efficiency on the size of the inhibitor molecule and the electronic distribution in the inhibitor molecule. With the rapid advancement of nanotechnology, thin films of thickness in the micron and nanometric scales are increasing their popularity in scientific and technological applications [10]. Nanoparticles have high tendency to interact with each other to form agglomeration [11]. Their unique properties are mainly due higher surface area of the nanosized particles in compare to microsized caused by their large surface area to volume ratio [12]. There are various reports concerning improving corrosion resistance using nanoparticles such as; TiO<sub>2</sub> [13], Cu<sub>2</sub>O [14], ZnO [15], ZrO<sub>2</sub> nanoparticles [16], Fe<sub>3</sub>O<sub>4</sub> [17], SiO<sub>2</sub> [18] organoclay [19] and Au nanoparticles [20]. The corrosion inhibition of the self-assembled Au, and Ag nanoparticles films on the surface of copper was studied [21]. They did reduction for H<sub>2</sub>AuCl<sub>4</sub> and AgNO<sub>3</sub> separately with NaBH<sub>4</sub> in an aqueous solution and used sodium oleate as stabilizer. Generally, various stabilizers (surfactants, gemini surfactants, polymers, triblock polymers, proteins and carbohydrates) have been used in the synthesis and characterization of different shaped and sized of advanced silver nano materials [22, 23]. It is well known that bulk Ag cannot react with hydrochloric acid (HCl). It was found that Ag coated with poly (vinylpyrrolidone) nanoparticles have an unusually high chemical nanoreactivity in the reaction with hydrochloric acid [24]. Ag nanoparticles can react with hydrochloric acid to form AgCl, which cannot happen for the bulk or coarse grained Ag. In the present work, our aims directed to prepare dispersed coated silver nanoparticles to apply as corrosion inhibitors for carbon steel in acidic solution using various techniques. The idea of present work is to use silver modified nanoparticles with polymerizable surfactants as a dispersant for well dispersed silver nanoparticles and also as corrosion inhibitors in acidic media. The nanoparticles can absorb the surfactants during the preparation procedure and then slowly release them in contact with aqueous hydrochloric acid.

## 2. EXPERIMENTAL

### 2.1. Materials

Silver (I) oxide (AgO) and sodium borohydride (NaBH<sub>4</sub>) were purchased from Sigma-Aldrich and used as received. Noigen RN-10 (NRN-10; polyoxyethylene 4-nonyl -2-prpylene-phenol) nonionic reactive surfactant (Daichi Kogyo Seiyaku of Japan manufacture; Montello, distributor) was used as received. Maleic anhydride (MA), 4-dimethylamino pyridine (DMAP), chloroform were purchased from Aldrich and used as received.

### 2.2. Preparation of polyoxyethylene 4-nonyl -2-prpylene-phenyl maleate (NME)

NRN-10 (36.4 g, 0.05 mol) and hydroquinone (0.02 g) as inhibitor were dissolved in chloroform (25 mL) as a solvent. A solution of maleic anhydride (MA, 8.82 g, 0.09 mol) and 4-

dimethylamino pyridine (DMAP, 0.09 g) in chloroform (45 mL) was added to the reaction mixture. The reaction temperature increased at 60°C for 24 h with vigorous stirring. The reaction mixture was extracted and carefully washed with water (5x50 mL) after cooled to room temperature. The extracted mixture was evaporated in rotary evaporator to remove chloroform and (36.2 g, 88%) was obtained as yellowish brown oil.

### 2.3. Preparation of Modified silver nanoparticles

A simple method to prepare coated silver nanoparticles prepared through the reduction of Ag<sub>2</sub>O by NaBH<sub>4</sub> in the presence of modified NRN-10 or NME as a surfactant. The silver/amphiphilic dispersions were prepared according to the following general procedure: The modified NME (0.5 g in 100 mL) was dissolved in an organic solvent immiscible with water (preferably chloroform was used). Ag<sub>2</sub>O (380 mg) was added with stirring overnight in a closed flask excluding light made sure that silver ions after slowly dissociation of the Ag<sub>2</sub>O completely coordinate at the carboxylic group of NME (solution A). A solution B was prepared by dissolving an equivalent amount of NaBH<sub>4</sub> (molar ratio of Ag/NaBH<sub>4</sub> between 0.5 and 1.0); NaBH<sub>4</sub> (40 mg) into deionized water (50 ml) in distilled water. By bringing both solutions A and B together, the coordinated silver ions were reduced to silver atoms at room temperature. A stable two phase system without washing out of silver salt or precipitation of silver could be observed either by using chloroform (lower phase) as a solvent. After 30 to 60 min of slow stirring (varied with the amount of inorganic precursor employed) both phases were separated from one another to stop the reaction and to prevent possible unwanted side reactions. The yielded nanoparticles dispersions were stored in sealed bottles under ambient conditions and used as received for analysis as well as for preparation of corrosion inhibitor solutions.

### 2.4. Characterization of the prepared surfactants

<sup>1</sup>H-NMR spectra of the prepared polymers were recorded on a 400 MHz Bruker Avance DRX-400 spectrometer.

Transmission electron microscopy (TEM) micrographs were taken with a JEOL JEM-2100F field emission transmission electron microscope using an accelerating voltage of 200 kV.

Ultraviolet visible (UV-vis) absorption spectra were obtained with a Techcomp UV2300 spectrophotometer using quartz cuvettes with 1 cm optical path length for the measurement.

### 2.5. Electrochemical measurements

EIS impedance measurements were performed using a Solartron 1470E system (potentiostat/galvanostat) with Solartron 1455A as frequency response analyzer. Multistate software was used to run the tests, collect and evaluate the experimental data. Impedance tests were performed in 1M HCl with and without inhibitor. Ag/AgCl electrode was used as the reference and Pt electrode was used as the counter electrode. The working electrode was prepared from a carbon steel with

dimensions 1mm (width) x 10mm (length). The impedance data were analyzed and fitted with the simulation ZView 3.3c, equivalent circuit software.

### 3. RESULTS AND DISCUSSION

Nanometer-size noble metals such as Ag and Au with large specific surface areas exhibit notable properties which are different from their corresponding bulk materials [25]. Silver (Ag) is a noble metal with an inert chemical reactivity in its bulk form and is listed below hydrogen in the activity series of metals. It is well known that bulk Ag cannot react with hydrochloric acid (HCl). If the reaction between Ag nanoparticles and HCl can occur, the product will be silver chloride (AgCl), which is an insoluble precipitate and can be easily collected for characterization. It was previously reported that, high chemical reactivity of Ag nanoparticles was observed in the reaction with hydrochloric acid [24]. In the present work, we planed to prepare dispersed Ag coated nanoparticles in HCl aqueous solution to use as corrosion inhibitors for carbon steel in acid media. In this respect, polymerizable alkyl phenol ethoxylates (APEs) play important role in colloidal chemistry of polymer latex to stabilize the colloidal dispersions [26]. In this work, we modify NRN-10 thought esterification with MA as listed in scheme 1. The modified surfmers investigated here can be easily prepared by acylation of hydroxyl group of terminated polyoxyethylene moiety with dicarboxylic acid anhydrides. The acylation catalyst, 4-dimethylaminopyridine (DMAP), is highly recommended to complete the reaction. The polymerization inhibitor, hydroquinone, added to inhibit the polymerization of allylic C=C double bonds of NRN 10. We attempted to introduce the carboxylic acid group (or anhydride groups) into the oxyethylene chain end of polymerizable APEs to increase the functionality and polymerizable bonds and to increase the surface activity of these compounds. The molecular structures of the polymerizable NRN-10, and NME surfactants were confirmed by  $^1\text{H-NMR}$  spectroscopy.

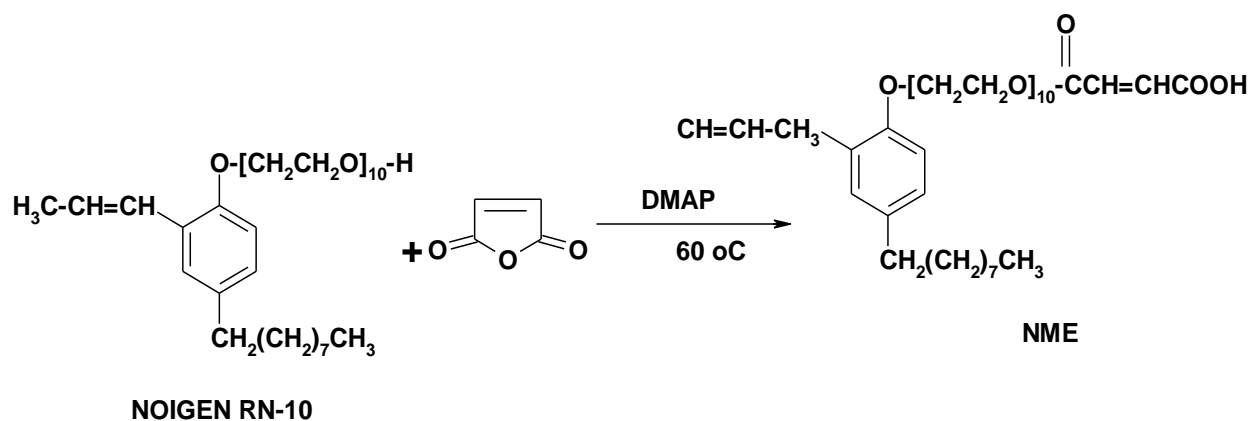


**Figure 1.** Modification scheme of NOIGEN RN-10.

Figure 1 shows the  $^1\text{H-NMR}$  spectra of NRN-10, and NME. The chemical shift values for all the modified Noigen surfactants are summarized in Table 1.

**Table 1.**  $^1\text{H}$  NMR chemical shifts, Spin splitting and integration of surfactants measured in  $\text{CDCl}_3$  with TMS as internal standard.

Peak	NOIGEN RN-10			NME		
	$\delta$ (ppm)	Spin splitting	Integration area	$\delta$ (ppm)	Spin splitting	Integration area
A	0.38	T	6.2	0.36	T	6.1
B	0.78	M	17.7	0.67	M	17.4
C	1.18	M	18.1	1.12	M	17.5
D	1.8	D	5.85	1.75	D	6.1
E	2.53	T	4.32	2.49	T	4.21
F	3.02	S	2.10	3.54	B	100
G	3.63	B	100	4.27	T	4.15
H	6.01	B	3.8	6.1	B	3.9
J	6.5-6.9	M	11.8	6.5-6.9	M	11.7
K	-	-	-	11.7	S	2.1
L	-	-	-			

The methylene triplet peak at 4.04 ppm due to  $-\text{CH}_2\text{OCO}$  attached to ester group also,  $-\text{COOH}$  moiety can be detected in NME spectra at 11.72 ppm. The disappearance of hydroxyl terminal group appeared at 3.02 ppm of NRN-10 indicated the acetylation and esterification of OH group. The methylene triplet peak at 3.65 – 3.72 ppm due to  $-\text{OCH}_2\text{CH}_2\text{O}-$  is shifted downfield. It was also determined that, the NME spectrum, Figure 2 b, proton resonance signals characteristic of double bond of maleic group were detected at  $\delta = 6.3 \pm 0.6$  ppm, and peak of methylene protons adjacent to oxygen atom of ester group were shifted downfield by  $\Delta\delta = 0.4 \pm 0.6$  ppm after acylation.

### 3.1. Preparation of silver coated nanoparticles

In the previous work [26], the data of surface activity for NME and NRN-10 indicated that the surface activity and adsorption increased with introducing MA at the end of NRN-10. The measurements confirm that the NME reduced the critical micelle concentration (cmc) value of NRN-10 and increased the concentration of surfactants adsorbed at the water–air interface, can be estimated as surface excess concentration  $\Gamma_{\text{max}}$ , and being the promising as polymerizable surfmer. The cmc was reduced from  $9.6 \times 10^{-4}$  to  $3.20 \times 10^{-4}$  mol/L, and  $\Gamma_{\text{max}}$  increased from  $1.62 \times 10^{-10}$  to  $1.97 \times 10^{-10}$  mol/cm<sup>2</sup> for NRN-10 and NME, respectively. These values indicated that the NME has strong adsorption affinity at interfaces more than NRN-10 which enforced to use as stabilizer to prepare Ag nanoparticles and to apply as corrosion inhibitors as illustrated in the experimental section. The hydrophilic NRN-10 core molecule needs to get a hydrophobic shell as NME to prevent a simple washing out of the encapsulated Ag nanoparticles. If NME is used as template to host inorganic silver nanospheres than the core diameter should limit the nanoparticle cluster growth during syntheses. We used NME bearing carboxylic group as a template to control the nanoparticles cluster growth and as a carrier for silver nanoparticles synthesized as described above. The intramolecular coordinated silver

ions ( $\text{Ag}^+$ ) were reduced to silver atoms ( $\text{Ag}^0$ ) by reaction with hydrogen and/or hydride ions ( $\text{H}_2$  and/or  $\text{H}^-$ ) resulting from the sodium tetrahydridoborate ( $\text{NaBH}_4$ ) used as reduction agent [27]. That means the described reaction gets only possible by interaction of the educts at the interface between both solutions as illustrated in the experimental section. The formation of metallic silver was observed by change of the color of the organic phase (solution A) while the aqueous phase (solution B) remains colorless. Furthermore the reduction of silver ions was verified by UV-Vis spectroscopy.

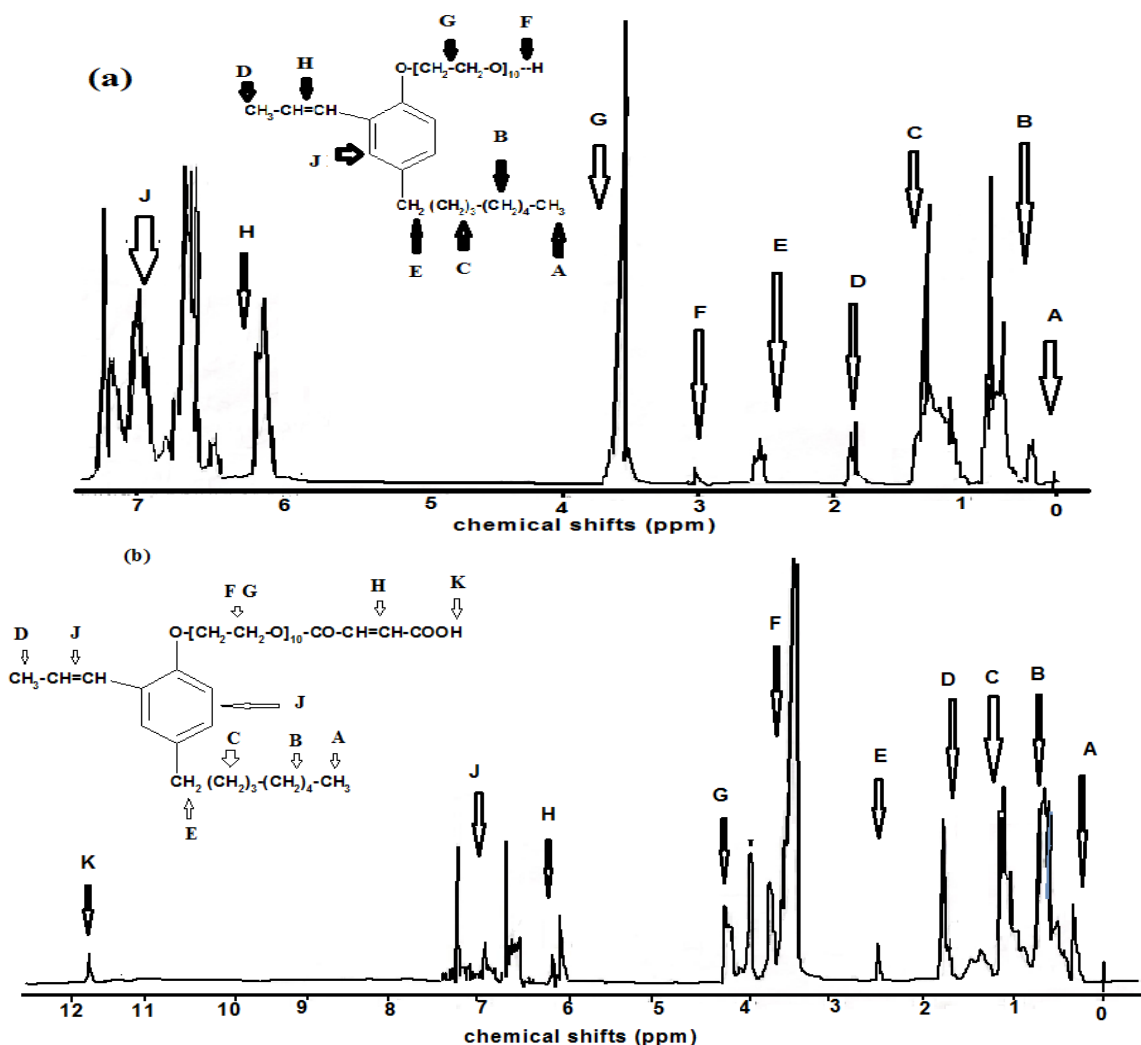


**Figure 2.**  $^1\text{H}$ NMR spectra of a) NOIGEN RN-10, and b) NME.

Figure 2 shows the UV-Vis spectrum of the 1M HCl aqueous solution for a small sample placed in a quartz crystal cuvette. The formation of nanosized silver spheres is observable in a strong increase in absorption at about 427 nm (2.9 eV), corresponding to the dipole resonance (plasmon resonance) of immediately-built silver nanoclusters [28].

The size and morphology of Ag nanoparticles prepared were investigated by TEM (Figure 3). Interestingly, no nanorods were detected. Figure 3 shows the TEM image of the Ag- nanoparticles, which are composed mainly of hexagonal shaped particles in presence of NME. Their grain sizes

measured from the micrograph range from 25 nm to 80 nm, and the mean grain size is 42 nm. Hexagonal plate-like Ag-nanoparticles have clear borders. The diameters of Ag nanoparticles (black spots) ranged from 2 to 18 nm.

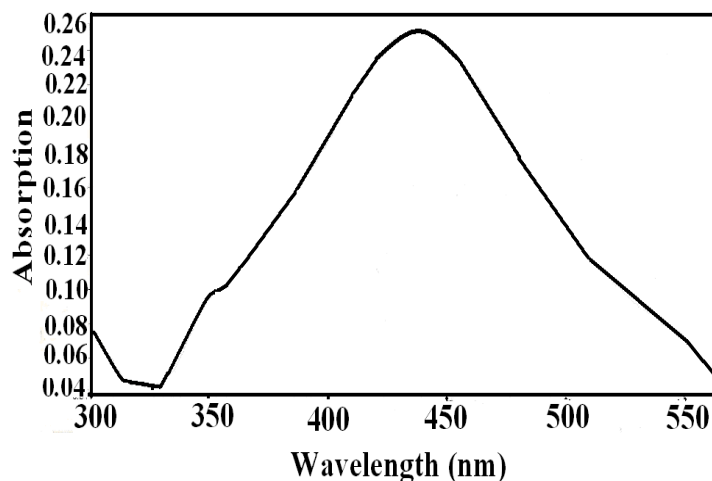


**Figure 3.** UV-vis absorption spectrum of 1M HCl aqueous solution of NME/Ag nanoparticles.

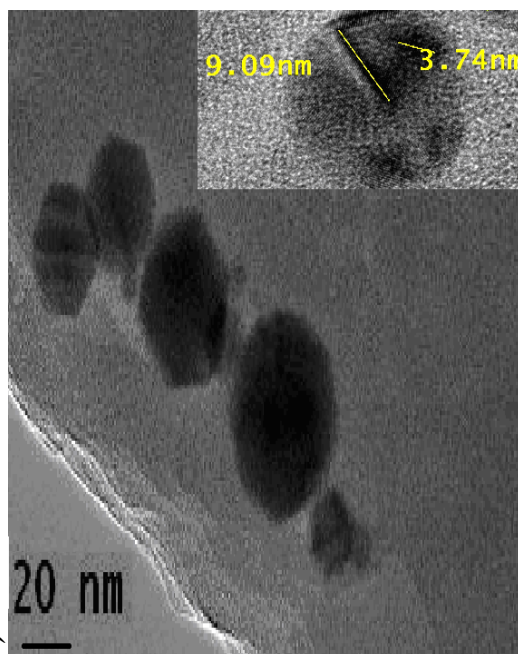


**Figure 4.** TEM image of NME/Ag nanoparticles.

The average diameter of Ag nanoparticles is 8.2 nm. The reasons for this morphology are not understood and may be due to interactions such as hydrogen bonding and electrostatic interactions between the NME head polar carbonyl group of NME molecules bound to the Ag nanoparticles. Formation of ion-pair and/or complexation between NME aggregates and  $\text{Ag}^+$  ions inhibits the all processes (nucleation, growth, adsorption and deposition) involved in the formation and stabilization

of metal nanoparticles. The lone pair electrons of oxygen atoms are responsible for the adsorption of NME on the positive surface of silver particles, which inhibit the growth, size and the reaction rate. The mechanism of the hexagonal silver nanoplate formation is not yet completely understood in presence of NME.

3.2 EIS measurement

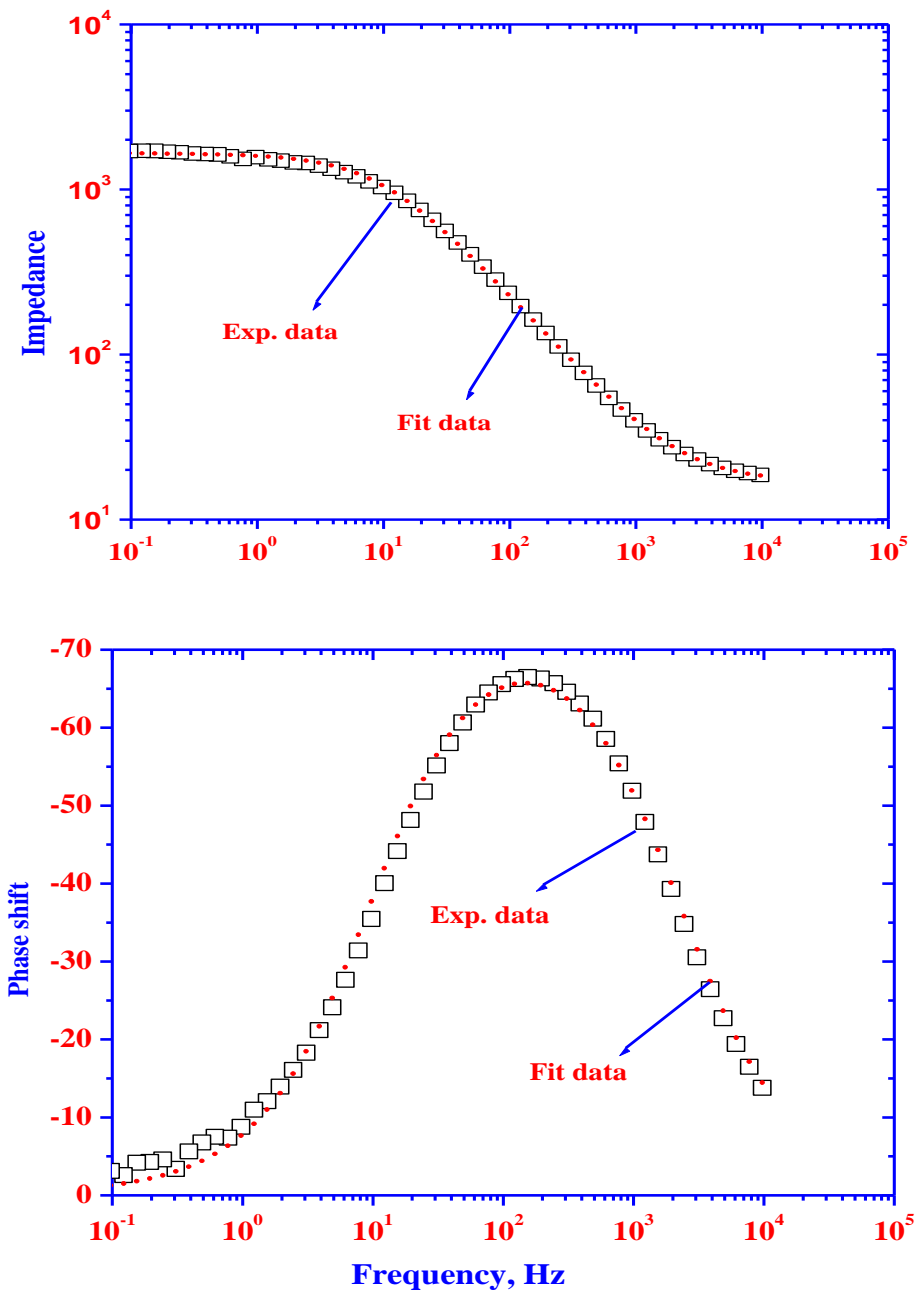
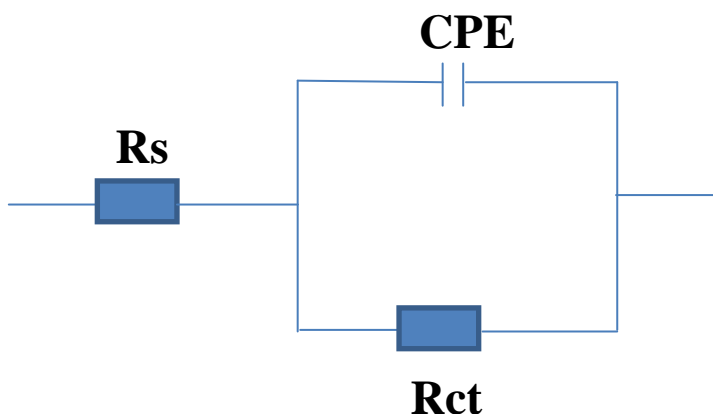


Figure 5. Bode diagram for carbon steel in 1 M HCl solution



**Figure 6.** Nyquist diagram for carbon steel in 1 M HCl solution.



**Figure 7.** Equivalent circuit used for fitting the impedance data in 1 M HCl solution.

Impedance measurements of the carbon steel electrode after 1 hour of immersion in 1M HCl solutions with and without inhibitor are performed over the frequency range from 10 KHz to 10 mHz. Impedance data in the form of Nyquist and Bode plots of carbon steel in 1M HCl without inhibitor are presented in Figs. 5-6, respectively. A single capacitive loop like semicircle, was observed in the absence of inhibitor and indicated that the corrosion process was controlled by charge transfer resistance, which depends either on direct electron transfer at the metal surface or on the electron conduction through the film surface [29]. It reflects the surface inhomogeneity of structural or interfacial origin, such as those found in adsorption processes [30]. Electrical equivalent circuits shown in Fig. 7 are generally used to model the electrochemical behaviour and calculate the parameters of interest such as electrolyte resistance ( $R_s$ ) and charge transfer resistance ( $R_{ct}$ ). In this case, the constant phase element, CPE, is introduced in the circuit instead of a pure double layer capacitor to give a more accurate fit [31-32] shown in Figures 5 and 6 for Nyquist and Bode plots, respectively in

case of blank solution. The CPE element is used to explain the depression of the capacitance semi-circle, which corresponds to surface heterogeneity resulting from surface roughness, impurities, dislocations, grain boundaries, adsorption of inhibitors, formation of porous layers [33-37]. The impedance function of a CPE has the following equation [38]:

$$Z_{CPE} = 1/A \times 1/(j\omega)^n \tag{1}$$

where A is the CPE constant,  $\omega$  is the angular frequency ( $\omega = 2\pi f$ , where  $f$  is the AC frequency), and  $j$  is the imaginary unit and  $n$  is a CPE exponent which can be used as a gauge of the heterogeneity or roughness of the surface [39]. The inhibition efficiency (IE) is calculated from:

$$IE = (1 - R_{ct} / R_{ct}^*) \times 100 \tag{2}$$

where  $R_{ct}^*$  and  $R_{ct}$  are the charge-transfer resistances with and without inhibitors, respectively. After the addition of an inhibitor in the blank solution the impedance of the electrode has significantly changed as shown in Figures 8-9 for Bode and Nyquist plot, respectively. It is clear that the diameters of the semi-circles in Nyquist plots increased with increasing inhibitor concentrations and is accompanied by an effective inhibition of the corrosion process due to the formation of the protective film on the electrode surface. It is evident that the Nyquist plots are composed of two capacitive loops. The first loop present at high frequencies can be attributed to the charge transfer resistance ( $R_{ct}$ ), which could correspond to the resistance between the carbon steel surface and the outer Helmholtz plane [40].

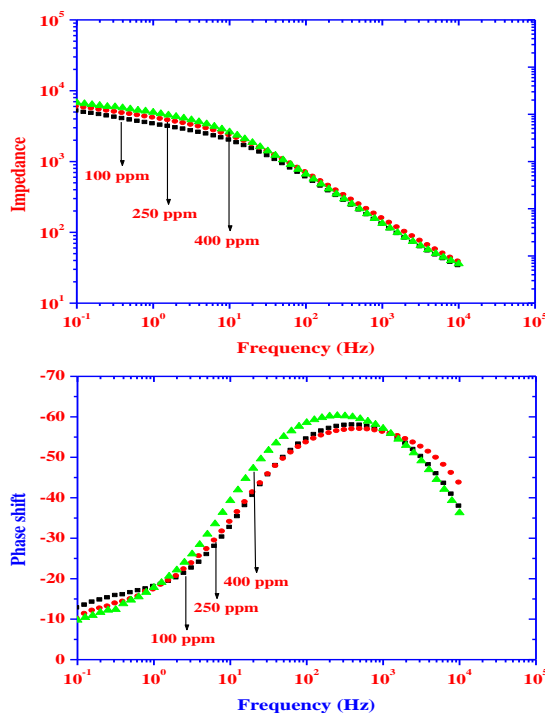


**Figure 8.** Bode diagram for carbon steel in 1 M HCl containing different concentration of inhibitors.

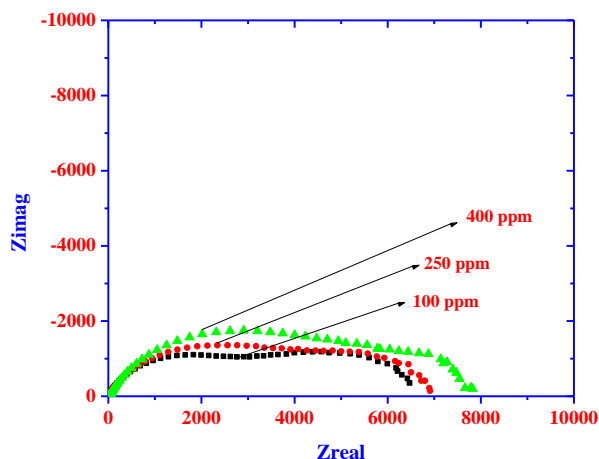


**Figure 9.** Nyquist diagram for carbon steel in 1 M HCl containing different concentration of inhibitors.

The second loop present at low frequencies is related to the film resistance, which can be ascribed to the adsorbed inhibitor molecules [41]. The remarkable increase in  $R_{ct}$  suggests that the amount of inhibitor molecules adsorbed on the carbon steel surface increases and consequently results in the decreasing of active sites necessary for the corrosion reaction. The equivalent circuit shown in Fig. 10 is used to simulate the experimental data.  $R_s$ , represents the solution resistance,  $R_{ct}$  is the charge transfer resistance and  $R_f$  represents the film resistance. The constant phase elements CPE1 and CPE2 are used to replace the double layer capacitance and the film capacitance, respectively.

The inhibition efficiency (IE) was calculated and listed in Table 2. It can be concluded that the inhibition efficiency of the inhibitor increases with increasing the inhibitor concentration with maximum inhibition efficiency observed at 400ppm concentration.

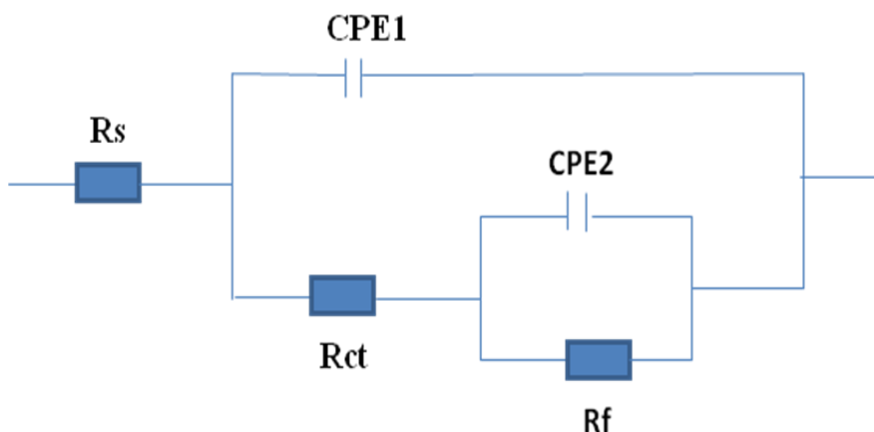


**Figure 10.** Equivalent circuit used for fitting the impedance data in 1 M HCl containing different concentration of inhibitors.

**Table 2.** Inhibition efficiency values for carbon steel in 1M HCl with different concentrations of silver nanoparticles.

Ag Nanoparticles Concentration (ppm)	% Inhibition Efficiency (IE)
100	70.259
250	73.690
400	76.683

#### 4. CONCLUSIONS

1-A simple method was applied to prepare coated silver nanoparticles with polymerizable surfactants.

2- The size and the morphology of the nanoparticles has been examined by TEM. The prepared silver nanoparticles has size ranging from 25 to 80 nm, while the diameters ranging from 2 to 18 nm

3- The inhibition efficiency of silver nanoparticles increases with increasing concentrations and the maximum inhibition efficiency was observed at 400ppm concentration.

4- EIS data indicated that silver nanoparticles reduced drastically the corrosion rate of carbon steel and exhibit good performance as well as barrier property against the corrosion in HCl solution.

#### ACKNOWLEDGMENT

The project was supported by the Research Center, College of Science, King Saud University.

#### References

1. E.F. Moura, A.O.W. Neto, T.N.C. Dantas, H. Scatena Jr., A. Gurgel, *Colloids Surf. A: Physicochem. Eng. Aspects* 340 (2009) 199.
2. D.M. Brasher, A.D. Mercer, *Br. Corros. J.* 3 (3) (1968) 120.
3. S. Yao, X. Jiang, L. Zhou, Y. Lv, X. Hu, *Mater. Chem. Phys.* 104 (2007) 301.
4. R. Solmaz, G. Kardas, M.C. ulha, B. Yazici, M. Erbil, *Electrochim. Acta* 53 (2008) 5941.
5. A M Atta, GA El-Mahdy, H S. Ismail and H A. Al-Lohedan, *Int. J. Electrochem. Sci.*, 7 (2012) 11834.
6. A M Atta, G A El-Mahdy, A A. Al-Azhary and H A. Al-Lohedan, *Int. J. Electrochem. Sci.*, 8 (2013) 1295.
7. M.A. Quraishi, R. Sardar, *Mater. Chem. Phys.* 78 (2002) 425.
8. J.M. Bastidas, P. Pinilla, J.L. Polo, S. Miguel, *Corros. Sci.* 45 (2003) 427.
9. M.A. Migahed, A.M. Abdul-Raheim, A.M. Atta, W. Brostow, *Materials Chemistry and Physics* 121 (2010) 208.
10. P. Farguez, F. Avilés, A.I. Oliva, *Surf. Coat. Technol.* 202 (2008) 1556.
11. M. Sabzi, S.M. Mirabedini, J. Zohuriaan-Mehr, M. Atai, , *Prog. Org. Coat.* 65 (2009) 222.
12. M. Yiu-Wing, Y. Zhong-Zhen, *Polymer Nanocomposites*, Wood head Publishing Limited, Cambridge, 2006.
13. O. Zubillaga, F.J. Cano, I. Azkarate, I.S. Molchan, G.E. Thompson, P. Skeldon, *Surf. Coat. Technol.* 203 (2009) 1494.
14. G. Gao, H. Wu, R. He, D. Cui, *Corros. Sci.* 52 (2010) 2804.

15. X. Zhang, F. Wang, Y. Du, *Surf. Coat. Technol.* 201 (2007) 7241.
16. M. Behzadnasab, S.M. Mirabedini, K. Kabiri, S. Jamali, *Corros. Sci.* 53 (2011) 89.
17. A.M. Atta, O.E. El-Azabawy, H.S. Ismail, M.A. Hegazy, *Corros. Sci.* 53 (2011) 1680.
18. Y. Li, P. S. Fedkiw, *Electrochimica Acta* 52 (2007) 2471.
19. T.A. Truc, T. T. X. Hang, V. K. Oanh, E. Dantras, C. Lacabanne, D. Oquab, N. Pébère, *Surf. Coat. Technol.* 202 (2008) 4945.
20. Z. Zhang, S. Chen, H. Ren, J. Zhou, *Applied Surface Science* 255 (2009) 4950.
21. D. Li, S.Chen, S. Zhao, H. Ma, *Colloids and Surfaces A: Physicochem. Eng. Aspects* 273 (2006) 16.
22. S. A. AL-Thabaiti, M. A. Malik, A. A. O. Al-Youbi, Z. Khan, J. I.Hussain, *Int. J. Electrochem. Sci.*, 8 (2013) 204.
23. C. Burda, X. Chen, R. Narayanan, M. A. El-Sayed, *Chem. Rev.* 105 (2005) 1025; (b) M. Harada, Y. Inada, M. Nomura, *J. Colloid Interface Sci.* 337 (2009) 427; (c) N. R. Jana, L. Gearheart, C. J. Murphy, *Adv. Mater.* 13 (2001) 1389;(d) P. Vasileva, B. Donkova, I. Karadjova, C. Dushkin, *Colloids Surfaces A: Physicochem. Eng. Aspects*, 382 (2011) 203;(e) J. Gao, C. M. Bender, C. J. Murphy, *Langmuir* 19 (2003) 9065;(f) Z. Khan, S. A. AL-Thabaiti, A. Y. Obaid, Z. A. Khan, A. O. Al-Youbi, *J. Colloid Interface Sci.*367 (2012) 101-108; (g) P. Raveendran, J. Fu, S.L. Wallen, *J. Am. Chem. Soc.* 125 (2003)13940.
24. L. Li, Y-J. Zhu, *J Colloid Interface Sci.* 303 (2006)415.
25. G. Schmid, *Chem. Rev.* 92 (1992) 1709.
26. A.M. Atta, A.K. F.Dyab, H.A. Allohedan, *J Surf and deterg* (2013)  
<http://link.springer.com/article/10.1007/s11743-012-1413-5>
27. M.Gladitz, S.Reinemann, H-J. Radusch, *Macromol. Mater. Eng.* 2009, 294, 178–189
28. G. Chumanov, D. D. Evanoff, *J. Phys. Chem. B* 2004, 108, 13962.
29. P.C. Okafor, C.B. Liu, X. Liu, Y.G. Zheng, *J. Appl. Electrochem.* 39 (2009) 2535–2543.
30. R.S. Goncalves, D.S. Azambuja, A.M. Serpa Lucho, *Corros. Sci.* 44 (2002) 467.
31. F. Mansfeld, M.W. Kendig, W.J. Lorenz, *J. Electrochem. Soc.* 132 (1985) 290.
32. F. Mansfeld, M.W. Kendig, *Werkst. Korros.* 34 (1983) 397.
33. A. Popova, E. Sokolova, S. Raicheva, M. Christov, *Corros. Sci.* 45 (2003) 33.
34. F.B. Growcock, J.H. Jasinski, *J. Electrochem. Soc.* 136 (1989) 2310.
35. U. Rammet, G. Reinhart, *Corros. Sci.* 27 (1987) 373.
36. A.H. Mehaute, G. Grep, *Solid State Ionics* 9–10 (1983) 17.
37. E. Machnikova, M. Pazderova, M. Bazzaoui, N. Hackerman, *Surf. Coat. Technol.* 202 (2008) 1543.
38. R. Macdonald, D.R. Franceschetti, in: J.R. Macdonald (Ed.), *Impedance Spectroscopy*, Wiley, New York, 1987, p. 96.
39. D.A. Lopez, S.N. Simison, S.R. de Sanchez, *Electrochim. Acta* 48 (2003) 845.
40. M. Ozcan, I. Dehri, M. Erbil, *Appl. Surf. Sci.* 236 (2004) 155.
41. F. Bentiss, M. Lagrenee, M. Traisnel, J.C. Hornez, *Corros. Sci.* 41 (1999) 789.